CONDUCTOR ANALYSIS OF THE ITER FEAT POLOIDAL FIELD COILS DURING A PLASMA SCENARIO

S. Nicollet [1] , P. Hertout [1] , J.L. Duchateau [1] , A. Bleyer [1] , D. Bessette [2]

[1] Département de Recherches sur la Fusion Contrôlée, Association Euratom-CEA, CEA/Cadarache, F-13108 Saint Paul- lez-Durance, France

[2] ITER-EDA Naka Joint Work Site, Japan

ABSTRACT

In the framework of the ITER (International Thermonuclear Experimental Reactor) FEAT (Fusion Energy Advanced Tokamak) project, a fully superconducting PF (Poloidal Field) system has been designed in detail. The Central Solenoid and the 6 equilibrium coils constituting the PF system provide the magnetic fields which develop, shape and control the 15 MA plasma during the 1800 s of a typical plasma scenario. The 6 PF coils will be wound two-in-hand from a 45 kA niobium-titanium CICC (Cable-In-Conduit-Conductor). These coils will experience severe heat loads specially during the 400 s of the plasma burn: nuclear heating due to the 400 MW of fusion power, thermal radiation and AC losses (30 to 300 kJ). The AC losses along the PF coil pancakes are deduced from accurate magnetic field computations performed with a 3D magnetostatic code, TRAPS. The nuclear heating and the thermal radiation are assumed to be uniform over a given face of the PF coils. These heat loads are used as input to perform the thermal and hydraulic analysis with a finite element code, GANDALF. The temperature increases (0.1 to 0.4 K) are computed, the margins and performances of the conductor are evaluated.

INTRODUCTION

The 6 PF coils of ITER FEAT Reactor (FIGURE 1) are manufactured in double pancakes of a thick-wall stainless steel square conductor, which provides the main structural material [1]. The PF coils are subject to pulsed loads with large variations of field within each machine cycle and they have to withstand safely all operational conditions, including plasma disruptions and fast discharges. The PF coils are designed based on a redundancy philosophy which allows the PF coil to operate with full current in case of a failure of one of the double pancakes. The PF coils are wound in separate modules and two-in-hand from a 45 kA NbTi Cable In Conduit Conductor (FIGURE 2) with 6 sub-cables arranged around a central cooling channel.

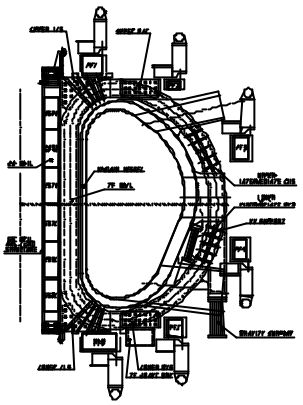

FIGURE 1. Poloidal field coils of ITER-FEAT reactor

SIMULATION MODEL AND CONDITION

In the following, main attention has been paid to coil PF6 which experiences the highest field and therefore takes advantage of NbTi at its limits. The scenario taken into account is referenced as No2 scenario.

NbTi Choice For The PF Coils

By using NbTi superconductor, cooled by supercritical helium, a substantial cost compared to Nb_3Sn is saved and the elimination of a reaction heat treatment greatly simplifies the insulation of such large diameter coils. In the framework of the PF Coils design and R&D activity, current density variations with magnetic field and temperature were investigated [2] for two candidate strands (Alstom and Europa Metalli) and correlated to the classical NbTi scaling laws. A precise J_c correlation is useful for determination of the electromagnetic characteristics, specially the current sharing temperature T_{cs} and the ΔT_{margin} we want to evaluate. According to these recent studies a more realistic critical temperature has been used in the model : Tc=6.85 K instead of Tc=7.17 K at 5 T as specified in ITER-FEAT design.

Total PF Coils Losses : AC Losses, Nuclear Heating And Thermal Radiation In The Conductor And Joule Heating And AC Losses In The Joint

Operation of the PF Coils according to scenario N°2 (FIGURE 3) are presented. PF6 operates at the highest field values with a maximum induction of 5.65 T and a maximum current of 40 kA (FIGURE 4).

FIGURE 2. Square Cable In Conduit conductor

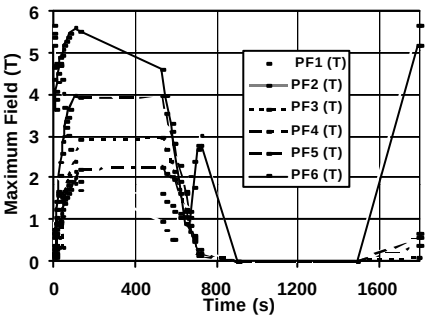

FIGURE 3. Maximum PF coils magnetic field

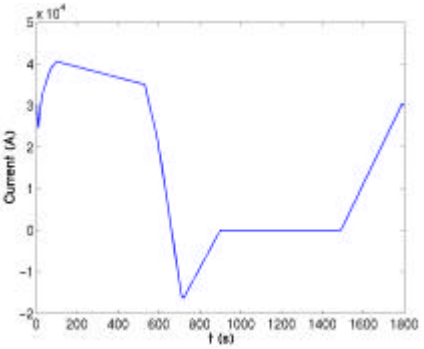

FIGURE 4. PF6 coil current

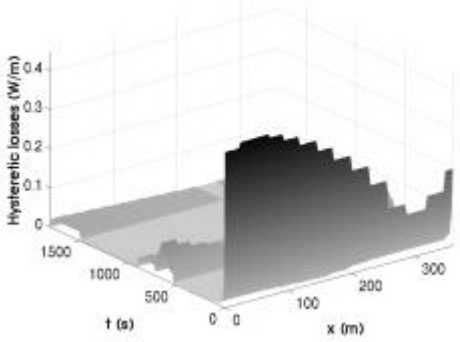

FIGURE 5. Hysteretic losses for a PF6 coil regular pancake

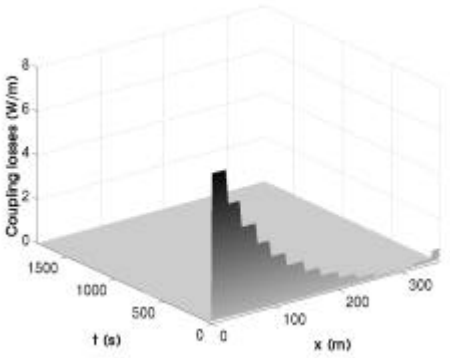

FIGURE 6. Coupling losses for a PF6 coil regular pancake

AC Losses

For this calculation [3] the coupling current time constant ($\pi\tau$) has been taken equal to 50 ms and the effective diameter for hysteretic losses has been taken equal to 5µm. The PF6 Coil sees during the 1800s of plasma scenario N°2, the maximum energy deposition compared to the other PF Coils ; this energy amounts to 3.44 and 110 kJ for coupling losses and 6.15 and 197 kJ for hysteretic losses, respectively for one conductor of the two-in-hand regular PF6 coil pancake and for the whole PF6 coil.

Nuclear Heating

Nuclear heating in the PF coils is concentrated on the coils facing the 3 main access ducts. The heat will be assumed to be all deposited in the top and/or bottom pancake or in the inner layer of conductors. The total nuclear heating on PF coils amounts to 395 W and the total nuclear heating on the magnet system (including the Central Solenoid and the Toroidal Field systems) is then 14.1 kW. On the PF6 Coil, the total energy deposition over scenario N°2 is 6 kJ. The total heat for each of the coil faces is as follows:

TABLE 1. Nuclear heating in the PF coils

	Top Face (W)	Inner Face (W)	Outer Face (W)	Bottom Face (W)
PF1	-	-	1	-
PF2	-	-	-	12
PF3	18	5	-	18
PF4	58	15	-	58
PF5	131	32	32	-
PF6	15	-	-	-

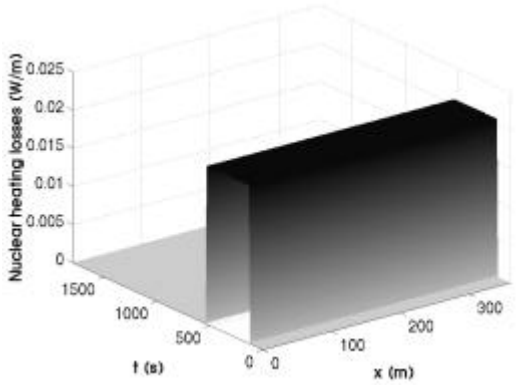

FIGURE 7. Nuclear heating for a PF6 coil regular pancake

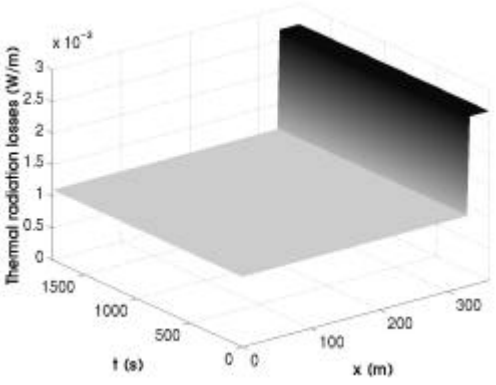

FIGURE 8. Thermal radiation losses for a PF6 coil regular pancake

TABLE 2. Thermal radiation on the protective case of the PF coils

	Top Face (W)	Inner Face (W)	Outer Face (W)	Bottom Face (W)
PF1	12	-	78	-
PF2	30	-	142	5
PF3	113	30	201	76
PF4	76	17	155	145
PF5	6	-	21	8
PF6	-	-	8	8

Thermal Radiation

Heat loads due to thermal radiation from the thermal shields or due to thermal conduction through the supports are considered as steady state heat loads for the analysis. The thermal radiation on the PF coils supports amounts to 1.1 kW and the heat radiated on the protective case in between the PF coils supports is distributed as shown in TABLE 2. For conductor thermal-hydraulic analysis purpose, it is assumed that 10% of this heat goes to the PF coils. On the PF6 Coil, the total energy deposition over scenario N°2 is 28.8 kJ.

Joule Heating And AC Losses In The Joint

The heat deposition in the joint (L_{joint} = 0.5 m) depends on the joint resistance r(t) [4], the magnetic field B(t) and the current I(t). FIGURE 9 presents the total energy deposition in the joint including the AC losses and the resistive losses as presented in [5]. FIGURE 10 presents the different sources of power deposition along the PF6 regular pancake conductor.

The Thermal-Hydraulic Simulation Model And The External Cooling Circuit Model

The complexity of the real thermal-hydraulic circuit is such that we have chosen to model and simulate only one flow path in detail by flow simulator (GANDALF, FLOWER) [6, 7] : one of the two-in-hand conductor chosen as the representative winding. The 1-D model consists of a maximum of four independent components at different thermodynamic states : the strands, the conduit, the bundle helium and the hole helium.

The detailed time and space distributions of all the losses are used as input. The magnetic field distribution and operating electric current are defined by the chosen test scenario. The heat exchange between pancakes and between adjacent conductors of the same pancake is not taken into account. Operating conditions are summarised in TABLE 3 [8] and parameters of PF conductor are given in [9] and in TABLE 4.

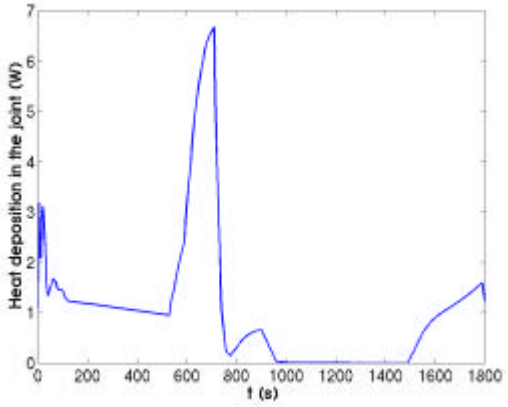

FIGURE 9. Total power deposition in the joint

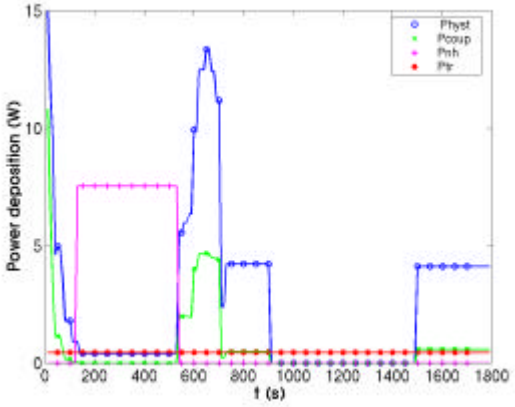

FIGURE 10. PF6 regular pancake power deposition

TABLE 3. PF operating conditions

	PF1	PF6	PF2	PF3	PF4	PF5
Nominal Peak Current (kA)	44.5	40.6	24.5	35.6	28.1	35.4
Nominal Peak Field (T)	5.65	5.59	1.88	2.94	2.25	3.97
Operating temperature at inlet (K)	4.6					
Initial pressure at inlet (MPa)	0.6					
Initial pressure at outlet (MPa)	0.5457					
Total pressure drop (MPa)	0.0543					

TABLE 4. Parameters of PF conductor

	PF1	PF6	PF2	PF3	PF4	PF5
Conductor hydraulic length (m)	196	361.5	280	442	403.5	363.5
Number of Turns x	15.75	26.75	10.70	11.75	10.75	13.75
Number of Conductors	x 16	x 16	x 10	x 16	x 16	x 16
Cable diameter (mm)	38.2			34.5		35.4
Central spiral od x id (mm)	12 x 10			12 x 10		12 x 10
Local void fraction in Bundle (%)	34.5			34.2		34.3
Superconducting NbTi Area (mm^2)	241.3			47.6		84.8
Jacket (Steel) Area (mm^2)	1748.4			1800.5		1709.4
Total Cu Area (mm^2)	386.1			449.7		442.5
Helium Area in Annulus (mm^2)	351.1			277.3		294.8
Total Helium Area (mm^2)	429.6			355.8		373.3
SC strand total twisted perimeter (m)	3.390			2.034		2.508
Hydraulic Diameter of Bundle (m)	0.4143			0.5453		0.4702

The connection of the PF6 coil conductor to the cryoplant is as shown in FIGURE 11. The conductor is cooled by 4.6 K and 0.6 MPa supercritical He in a closed circulation loop with an imposed pressure at the outlet of the conductor (maintained by a relief reservoir). Under normal pulse operating conditions, there is no helium flow in or out of this loop. Parameters (technical data) of cryoplant and components (pipes, pumps, heat exchangers, reservoir and valves) are listed in TABLE 5.

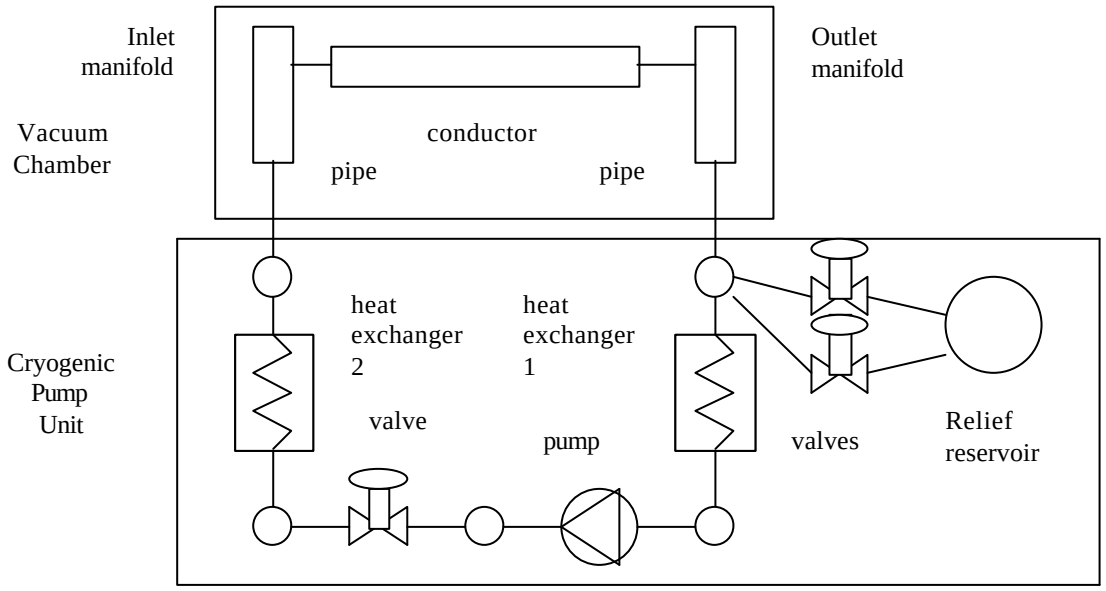

FIGURE 11. Calculation model of PF6 conductor and cryoplant

TABLE 5. Parameters of cryoplant

Total helium volumes / manifold volume (10^{-4} m^3)	2.05 / 1
2 Pipes length (m) / section (m^2) / diameter (m) / friction factor	10 / 10^{-4} / 3 10^{-3} / 1
Relief reservoir volume (m^3) / pressure (MPa) / temperature (K)	1000 / 0.5457 / 4.6
2 Heat exchangers length (m) / section (m^2) / diameter (m)/ friction factor / wetted perimeter (m) / wall temperature (K)	5 / 3 10^{-4} / 3 10^{-3} / 1 / 0.1 / 4.6
Volumetric pump length (m) / section (m^2) / mass flow rate (g/s)	1 / 3 10^{-4} / 9.9 10^{-3} (PF6)
Check valve length (m) / section (m^2) / pressure drop (MPa)/ friction factor	1 / 3 10^{-4} / 0 / 5 (pump) and 0.01(reservoir)

SIMULATION RESULTS AND DISCUSSION

With the operating conditions (TABLE 3), the initial supercritical helium inlet density is ρ_{He} = 138 kg/m^3. The total helium mass flow rate in all the PF coils is 1.8 kg/s. TABLE 6 summarises the different mass flow rates m flowing in each parallel conductor (hydraulic length L and helium cross section AHe) of the different coils and the transit time t of helium along the conductor calculated without heat loads from the mass flow rate and average velocity U as follow : $U = m / (\rho_{He}.AHe)$ $t = L / U$

The analysis performed allows estimation of the temperature and pressure rises, the helium flow and the ΔT_{margin} in the N°2 operating scenario. Here are presented the results for a PF6 regular conductor (exactly the 11th conductor) which sees the maximum magnetic field. Concerning the heat loads, we added to the maximum AC Losses of this particular conductor the nuclear heating load on the top face (TABLE 1, FIGURE 7) and the thermal radiation load on the bottom face (TABLE 2, FIGURE 8), supposing these steady loads are transmitted by conduction to the regular pancake studied. This case is very conservative and in reality the load of this pancake is lower.

TABLE 6. PF Coils mass flow rate and transit time without heat loads

Mass flow rate and transit time	PF1	PF6	PF2	PF3	PF4	PF5
Mass flow per unit conductor (g/s)	14.14	9.9	11.24	8.67	9.13	9.5
Total mass flow per coil (g/s)	452.48	316.8	224.8	277.44	292.16	304
Total Helium Area (mm^2)	429.6	429.6	355.8	355.8	355.8	373.3
Average helium velocity (m/s)	0.238	0.166	0.228	0.176	0.185	0.184
Transit time along conductor (s)	824	2170	1226	2509	2175	1976

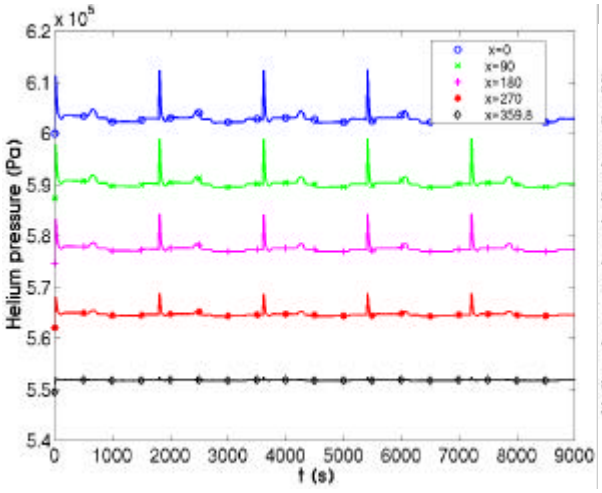

FIGURE 12. Pressure rise in a PF6 regular pancake during 5 successive plasma scenari

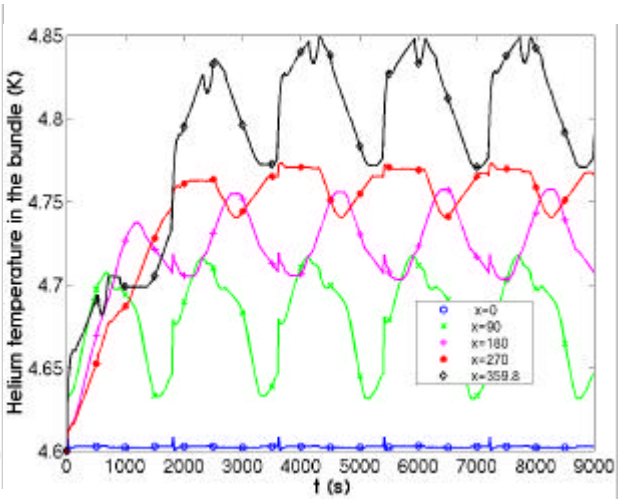

FIGURE 13. Temperature rise in a PF6 regular pancake during 5 successive plasma scenari

With the previous assumption and taking into account the geometric parameters of the conductor, the pressure and temperature rises are certainly conservative. A negligible pressure rise (nearly 0.1 bar) is observed (FIGURE 12) at the inlet of the conductor. Concerning the temperature (FIGURE 13), a steady state regime is reached from the 3rd plasma scenario. The peak helium temperature (for both bundle and hole) is observed at the outlet (x=359 m) with a maximum of 4.85K. The pressure and temperature rises are smaller for the other pancakes (typically 4.75 K and less than 0.61 MPa for PF1).

The counter flow heat exchange existing in the joint can not be simulated by GANDALF. The joint behaviour has been checked and been judged acceptable in a previous report [10] assuming a joint inlet temperature of 5K – temperature never reached according to this conductor simulation.

Time dependence of the conductor inlet and outlet mass flow rate is also presented (FIGURE 14). The mass flow rate is at the nominal value near the inlet of the conductor and is maximum at the outlet; this is due to helium expansion during heating. The expansion is important at the outlet because of helium temperature rise during plasma scenario. The model with relief reservoir introduces an artificial asymmetry between inlet and outlet for the pressure and the mass flow. The current sharing temperature T_{cs} and the critical current density J_c are related as follows, where S_{nonCu} is the superconductor cross section, B, T and I the operating magnetic field, temperature and current. The ΔT_{margin} is defined as the difference between the current sharing temperature and the operating temperature [11]. FIGURE 15 shows the evaluation of this parameter : it varies between 2.5 and 4K during plasma scenario and only at the begin of each scenario reaches the minimum value of 1.8K at the inlet of conductor where B is maximum.

$$S_{nonCu}.J_c.(B(x,t),T_{cs}(x,t)) - I(t) = 0$$

which gives $T_{cs}(x,t)$

$$\Delta T_{margin} = T_{cs}(x,t) - T(x,t) \geq 1.5K$$

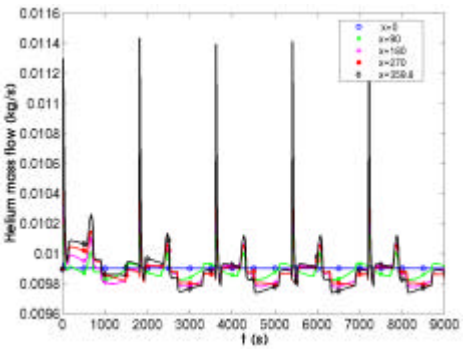

FIGURE 14. Mass flow rate in a PF6 regular pancake during 5 successive plasma scenari

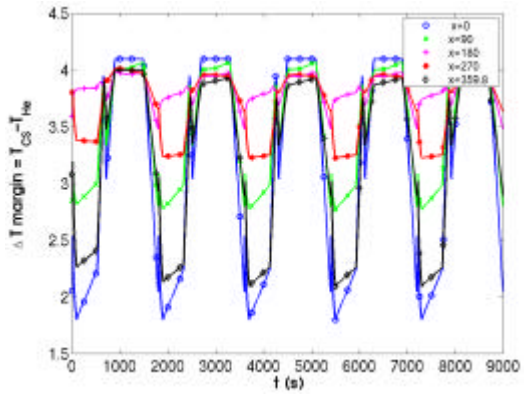

FIGURE 15. ΔT_{margin} in a PF6 regular pancake during 5 successive plasma scenari

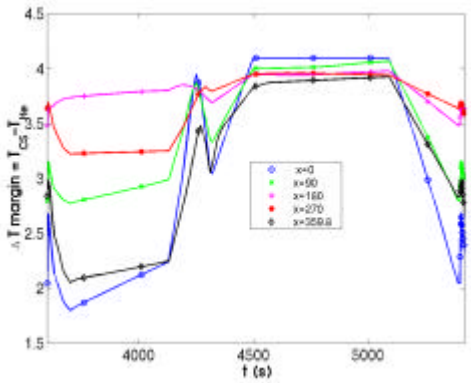

FIGURE 16. ΔT_{margin} in a PF6 regular pancake during the 3rd plasma scenario

For the PF1 coil, the ΔT_{margin} is 1.75 K because of the slightly higher current (43 kA). In FIGURE 16, we focus on the 3rd plasma scenario where the steady state regime is reached with the most critical (minimum) ΔT_{margin}. A very important design criterion of the PF coil is that a ΔT_{margin} of 1.5 K has to be satisfied at any time and in any place of the coil. Such a specification can be checked only after such a thermal-hydraulic analysis taking into account all the input loads.

CONCLUSION

A conservative thermal-hydraulic analysis of the conductor of an ITER-FEAT PF Coil has been performed by combining highest field values and maximum heat loads values (real AC losses on the conductor and maximal thermal radiation and nuclear heating transmitted by conduction). The pressure rise (0.1 bar) and temperature rise (0.4 K) observed during 5 pulses of plasma scenario are limited to acceptable values.

The ΔT margin (difference between current sharing temperature and operating temperature) is higher than 1.8 K. The criteria of 1.5 K is then respected at any time and position in the coil. This subsequently validates the choice of NbTi for all PF Coils, thanks to their lower field. The NbTi content for all the other coils will anyway be checked.

ACKNOWLEDGMENT

The GANDALF and FLOWER codes were developed by L. Bottura of Cryodata, whose assistance in these calculations is gratefully acknowledged. We thank very much also H. Takigami of Toshiba for collaboration. This work has been performed in the framework of the 00/541 Euratom contract.

REFERENCES

1. C. Sborchia and al., "Status of the ITER Magnet Design and Model Coils", in *IEEE Transactions on applied superconductivity*, vol. 10, No. 1, March 2000, pp. 554-559.
2. L. Zani and al., " Characterization of transport properties variations with magnetic field and temperature of ITER-candidate NbTi strands", to be published at EUCAS 2001 (Copenhaguen)
3. P. Hertout and al., "Heat Deposition in the ITER FEAT Poloidal Field Coils during a Plasma Scenario", to be published at the 17th Magnet Technology Conference – Geneva, Sept. 2001.
4. D. Ciazynski and al., "Test Results and Analysis of two european full-size Conductor Samples for ITER", in *IEEE Transactions on applied superconductivity*, vol. 10, No. 1, March 2000, pp.1058-1061.
5. D. Ciazynski and al., "Electrical and thermal designs and analyses of the joints of the ITER PF coils", to be published ar the 17th Magnet Technology Conference – Geneva, Sept. 2001.
6. L. Bottura and al., "A numerical Model for the simulation of Quench in the ITER Magnets", in *Journal of Computational Physics* 125, pp.26-41, 1996
7. L. Bottura and al., "Quench analysis of the ITER TF and CS coils using a solver of the cryogenic plant validated in the QUELL experiment", in *IEEE Transactions on applied Superconductivity* (ASC98) Vol.9, No. 2, pp. 616-619, 1999
8. ITER EDA Joint Central Team, Naka JWS, "Basic Design Package for Analysis, BDPA-2000", Version 2, 6 March 2000, Superconducting Coils & Structures Divison.
9. D. Bessette and al., "Conductors of the ITER Magnets", in *IEEE Transactions on applied Superconductivity* (ASC2000), Vol.11, No. 1, pp.1550-1553, 2000.
10. D. Ciazynski, P. Decool, P. Libeyre, A. Martinez, "ITER PF Coils Design and Analysis, CS Cooling Inlets", Intermediate report on phase 1 of EFDA Contract 00/541, 2001.
11. J.L. Duchateau, "Cable en Conduit Superconductors", Handbook of Applied Superconductivity, IOP, 1998, pp. 265-280.